

# Image Transfer by Modulation of Short Light Pulses

M. B. Danailov, I. P. Christov, and N. I. Michailov

Faculty of Physics, Sofia University, BG-1126 Sofia, Bulgaria

Received 30 January 1989/Accepted 6 April 1989

**Abstract.** This paper shows that the Fourier-processing based modulation of short laser pulses can be successfully used for all-optical image transfer. The system under consideration consists of a transmitter, where the transferred image modulates the frequency profile of a carrier pulse, and a receiver, where after the reverse processing an original image is restored. The main limitations are discussed and the information capacity of a single pulse is obtained. The results from preliminary experiments using a CPM-ring dye laser as a source of carrier pulses are presented.

**PACS:** 42.30.Va, 42.30.Qw, 42.60.By

In the recent years the idea of modulating short light pulses by spatial filtering of their optical frequency components has been studied both theoretically and experimentally [1–3]. One of the schemes based on this idea consists of a grating pair and a  $4-f$  optical processing system between the gratings. A mask with variable transmittance, inserted in the Fourier plane of the  $4-f$  system, performs the frequency modulation of the processed pulse. This relatively simple optical scheme allows one to obtain pulse modulation with a very high temporal resolution [3]. A promising area for the application of the said systems are optical communications. For example, a code-division, multiple-access optical communication system based on that principle for pulse modulation, is proposed in [4, 5].

In this paper we consider the possibility of using the Fourier-processing based modulation of short light pulses for all-optical image transfer. The theoretical analysis presented utilizes some results obtained in the recent paper [6]. Some preliminary experiments are discussed.

## 1. Analysis of the Proposed System

We will consider a system consisting of a transmitter and a receiver with some transparent medium between them (Fig. 1). The transmitter comprises two gratings  $G_1$  and  $G_2$ , situated at the front ( $F_1$ ) and the back ( $F_2$ )

focal planes of a conventional  $4-f$  optical processing system [7]. The image to be transferred is placed in the Fourier plane  $F \equiv F'_1 \equiv F_2$  of the  $4-f$  system as a mask with transparency function  $H(\kappa)$ . A broadband spectrum laser pulse is used as an information carrier. On passing the grating  $G_1$  the pulse is spectrally dispersed, so that the lens  $L_1$  forms in its back focal plane an image of the pulse spectrum: every frequency component is centered at a defined point in this plane. Consequently, the complex image  $H(\kappa)$ , placed in the plane  $F$ , modulates the frequency spectrum of the pulse. The second lens  $L_2$  and the grating  $G_2$  recollimate the radiation into a pulse with a new spectral structure (and therefore a new temporal profile), which carries an information about the image  $H(\kappa)$ . After propagating some distance through the transparent medium the modulated pulse enters the receiver, which consists of a grating  $G_3$  and an image sensor, placed at the front and at the back focal planes of the lens  $L_3$ , respectively. The function of the receiver is to restore the image at the input of the sensor.

Obviously, the mask  $H(\kappa)$  modulates not only the frequency but also the spatial structure of the passing field. Furthermore we will investigate the possibility of obtaining at the output of the transmitter a purely frequency-modulated field, keeping the Gaussian spatial profile of the initial pulse only slightly changed. This is necessary for two reasons:

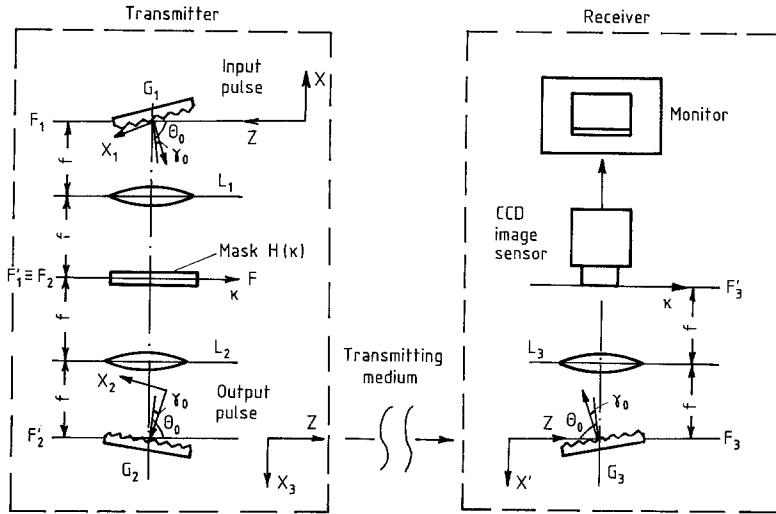


Fig. 1. Optical scheme of the image transfer system

1. The Gaussian spatial profile remains invariant along the free-space propagation and will allow an accurate image reconstruction in the receiver.

2. The Gaussian beam has the smallest (transverse extent)  $\times$  (angular divergence) product (see e.g. [8]), being therefore most suitable for a long distance transmission.

We will now analyze some aspects of the system operation. Following [6], we work in the plane  $(x, z)$ , where the axis  $z$  is chosen along the direction of propagation of the pulse and the  $x_j$  ( $j=1-3$ ) axes lie in the plane of the grating's dispersion.

Let the initial laser pulse be factorized at the input of the transmitter:

$$a_{\text{in}}(x, t) = a_0 \exp(-x^2/a^2) a_{\text{in}}(t),$$

where  $a_{\text{in}}(t)$  is the pulse envelope, and a Gaussian spatial profile is assumed with a width "a" at the  $e^{-1}$  level. In the frequency domain we have:

$$a_{\text{in}}(x, \omega) = a_0 \exp(-x^2/a^2) a_{\text{in}}(\omega),$$

where

$$a_{\text{in}}(\omega) = \int_{-\infty}^{\infty} a_{\text{in}}(t) \exp(-i\omega t) dt,$$

$\omega$  being the shift from the central frequency  $\omega_0 = 2\pi c/\lambda_0$ .

To account for the pulse passing through the gratings we use the formula [9]:

$$a_1(x_1, \omega) = b_1 a_{\text{in}}(\alpha x_1, \omega) \exp(ik\beta\omega x_1), \quad (1)$$

where  $a_1(x, \omega)$  is the field amplitude behind the grating. The abbreviations are as follows:  $\alpha = \cos(\theta_0)/\cos(\gamma_0)$ ,  $\beta = 2\pi c/[\omega_0^2 d \cos(\gamma_0)]$ ;  $\theta_0$  and  $\gamma_0$  are the angles of incidence and first-order diffraction on the grating,  $d$ -grating constant,  $c$ -velocity of light,  $k = \omega_0/c$ -light wavenumber,  $b_j$  ( $j=1-6$ )-constants accounting for the reflection and absorption losses. We shall use  $\alpha = 1$ .

The transfer of the pulse from the front to the back focal planes of the lenses is described by Fourier transform from  $x$ -space to the  $\kappa$ -space. Then, following [6] we find the field in the plane F:

$$a_2(\kappa, \omega) = b_2 a_{\text{in}}(\omega) \exp[-(\kappa - k\beta\omega)^2 a^2/4], \quad (2)$$

where  $\kappa = 2\pi x/\lambda_0 f$ . Multiplying the amplitude  $a_2(\kappa, \omega)$  by the mask transmittance  $H(\kappa)$  and accounting for the lens  $L_2$  and the grating  $G_2$ , we obtain the output field amplitude:

$$a_{\text{out}}(x_2, \omega) = b_4 a_{\text{in}}(\omega) \exp(ik\beta\omega x) \int_{-\infty}^{\infty} \times \exp[-(\kappa - k\beta\omega)^2 a^2/4 + ikx_2] H(\kappa) d\kappa, \quad (3)$$

It is seen that the function  $H(\kappa)$  is coded into the spectral-spatial structure of the output radiation.

We will suppose that along the propagation to the receiver the field characteristics change mainly due to diffraction. If the spatial profile of the transmitter output pulse  $a_{\text{out}}(x, \omega)$  is nearly Gaussian, the diffraction will cause only a beam expansion, which can be easily compensated by an appropriate telescopic system at the input of the receiver. Therefore, in this case we can consider that the diffracted field  $a_r(x', \omega)$  is equal to  $a_{\text{out}}(x, \omega)$  and is given by (3). Then, after again using (1) for the grating  $G_3$  and Fourier-transforming for the lens  $L_3$  we find the amplitude in the plane of the image sensor:

$$a_r(\kappa, \omega) = b_6 a_{\text{in}}(\omega) \exp[-(\kappa - k\beta\omega)^2 a^2/4] H(\kappa). \quad (4)$$

The pure spatial distribution, corresponding to  $a_r(\kappa, \omega)$ , is obtained after integrating the last formula over  $\omega$ :

$$a_r(\kappa) = H(\kappa) \int_{-\infty}^{\infty} a_{\text{in}}(\omega) \exp[-(\kappa - k\beta\omega)^2 a^2/4] d\omega. \quad (5)$$

In fact, the sensor will measure the intensity  $I_r(\kappa) \sim |a_r(\kappa)|^2$ , so that only the amplitude of  $H(\kappa)$  can be retrieved. The phase reconstruction in the case of a complex function  $H(\kappa)$  can be done with some additional design, using conventional optical methods for phase retrieval, e.g. interference of the modulated pulse with a reference pulse or so called “phase-contrast method” [10]. The integral which multiplies  $H(\kappa)$  in (5) can be calculated if the pulse spectrum  $a_{in}(\omega)$  is known and, if necessary, can be eliminated by optical or electronical filtering.

Formula (5) was obtained for the case when the modulated field (3) has nearly a gaussian spatial profile. Now we will discuss the conditions which assure that this assumption is valid. Equation (2) shows that the light field in the plane F can be considered as a superposition of different frequency components, each component having a Gaussian spatial profile with a width  $\delta\kappa_m = 2/a$  ( $\kappa$  units) and centered at a point  $\kappa = k\beta\omega$ . Integrating (2) over frequencies and supposing a Gaussian pulse envelope  $a_{in}(t) = a_0 \exp(-\alpha_0 t^2)$ , which corresponds to  $a_{in}(\omega) = a_0 \exp(-\omega^2/4\alpha_0)$  in the frequency domain, we obtain:

$$a(\kappa) = a_0 \exp[-a^2\kappa^2/4(1+R^2)],$$

where  $R = \alpha_0^{1/2} k\beta a$  is a dimensionless parameter, introduced in [6]. The last formula represents the total spot in the plane F: it is a Gaussian with a width  $\delta\kappa_{tot} = 2(1+R^2)^{1/2}/a$  in  $\kappa$  units. Next we will call  $\delta\kappa_m$  “a monochromatic spot size” and  $\delta\kappa_{tot}$  – “a total spot size”. It is seen that the greater  $R$ , the greater the ratio of the total to the monochromatic spot size:  $\delta\kappa_{tot}/\delta\kappa_m = (1+R^2)^{1/2}$ . We should note that in the case of a non-gaussian pulse spectrum  $a_{in}(\omega)$ , in the calculation of  $R$  the multiplier  $\alpha_0^{1/2}$  should be replaced by the spectrum halfwidth at the  $e^{-1}$  level.

If the function  $H(\kappa)$  varies slowly with  $\kappa$ , so that it could be considered as a constant for a distance on the order of  $\delta\kappa_m$ , the shape of every frequency component will be only slightly changed and therefore their superposition – the output field spatial profile, will remain nearly Gaussian. This fact is proved in [6]. Obviously, the above condition cannot be fulfilled if  $H(\kappa)$  is a binary image. In this case the diffraction on the edges will lead to the appearance of higher orders and to substantially non-gaussian spatial profiles of the frequencies, centered closer than  $\delta\kappa_m$  from the edges. Consequently, the single edge in the original image will appear smeared on the order of  $\delta\kappa_m$  in the restored image. For demonstration we have performed some computer simulations of the transfer of binary amplitude gratings with different periods. The results for two interesting cases are presented:

Case 1. Grating period  $1.5\delta\kappa_m$  – Figs. 2 and 4.

Case 2. Grating period  $4\delta\kappa_m$  – Figs. 3 and 5.

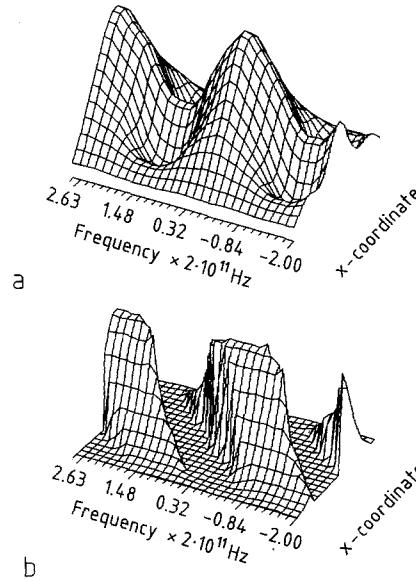


**Fig. 2a, b.** Intensity spectral-spatial distribution  $I(x, \omega)$  for  $H(\kappa)$  a binary grating with period  $1.5\delta\kappa_m$  (see Case 1 in the text): **a**  $I(x, \omega)$  at the transmitter output; **b**  $I(x, \omega)$  at the receiver input

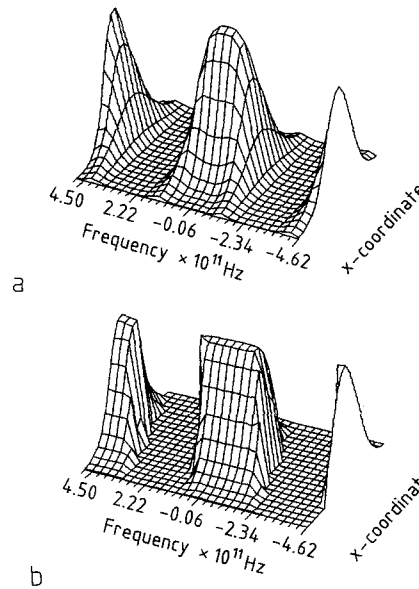


**Fig. 3a, b.** Intensity spectral-spatial distribution  $I(x, \omega)$  for  $H(\kappa)$  a binary grating with period  $4\delta\kappa_m$  (see Case 2 in the text): **a**  $I(x, \omega)$  at the transmitter output; **b**  $I(x, \omega)$  at the receiver input

Figures 2a and 3a show the intensity spectral-spatial distribution  $I(x, \omega) = |a(x, \omega)|^2$  at the output of the transmitter. Figures 2b and 3b show the same distribution at the receiver input, calculated from (3) using the Fresnel-Kirhoff integral in the far-zone approximation [7]. As it is seen, the strong deviation from the Gaussian shape, observed in Fig. 2a for Case 1, causes severe distortions of the field due to the diffraction (Fig. 2b). In result, the intensity spatial distribution in the plane of the sensor, shown in

Fig. 4b, differs considerably from the function  $H(\kappa)$  (Fig. 4a). In the Case 2 most of the frequency components of the transmitter's output field have a nearly Gaussian spatial profiles (Fig. 3a), the distortions of the field in the far-zone are smaller (Fig. 3b), and the original grating can be reconstructed from the field intensity distribution in the sensor plane, shown in Fig. 5b. As a consequence, when a binary image is transferred, the minimal size of the image pixels should

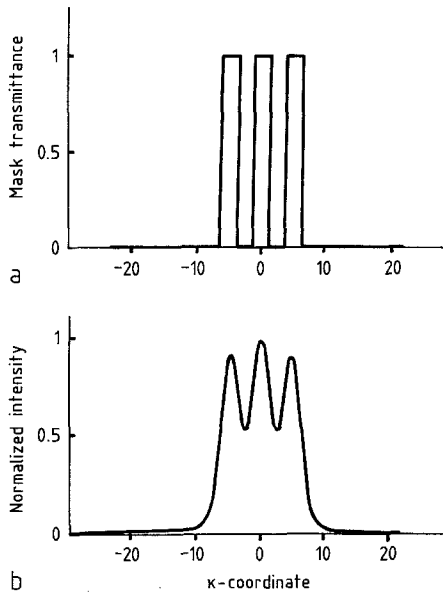


**Fig. 4.** **a** Plot of the mask transmittance  $H(\kappa)$ ; **b** plot of the intensity distribution at the input of the image sensor. Both plots are for Case 1 in the text

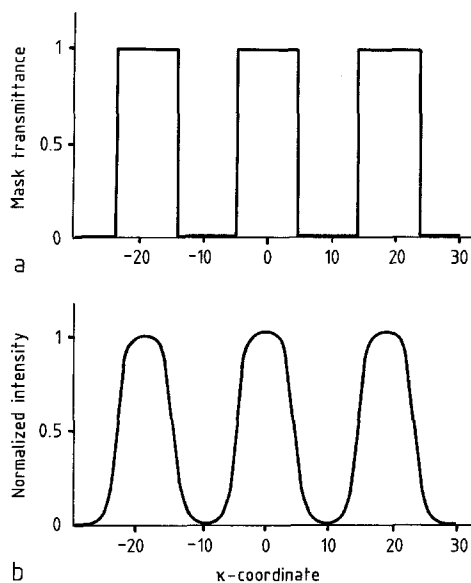


**Fig. 5.** **a** Plot of the mask transmittance  $H(\kappa)$ ; **b** plot of the intensity distribution at the input of the image sensor. Both plots are for Case 2 in the text

be at least  $2\delta\kappa_m$ . Since the full size of the transferred image cannot exceed the total spot size  $\delta\kappa_{tot}$ , the information capacity of a single pulse is about  $(1 + R^2)^{1/2}/2 \approx R/2$  bits.

The above considerations show that the source of carrier pulses for the proposed system should be chosen according to the following requirements: 1) A broad spectrum, which assures a large enough  $R$  value; 2) A good spatial coherence and a near Gaussian spatial profile; 3) A good stability of the spectrum. For the case of complex image transfer a well-defined phase relations between the different frequency components should be assured; 4) High repetition rate.

A convenient source that meets all the above requirements is the femtosecond dye laser. If only the amplitude image is transferred, a broadband cw dye laser, specially designed to assure a stable spectrum, can be used too.

### 2. Experimental

Our experimental setup was arranged according to Fig. 1, with a distance between the transmitter and the receiver of 1 m. A CPM-ring Rhodamine 6G dye laser was used as a source. The laser configuration was similar to that described in [11]. As a saturable absorber TCETI-tetrafluorborate was used [12]. This laser delivered pulses of about 110 fs duration at a repetition rate 100 MHz. The pulse spectrum was slightly asymmetrical, with FWHM about 1.5 nm (see Fig. 6a). The beam diameter was expanded to  $a = 2$  cm.

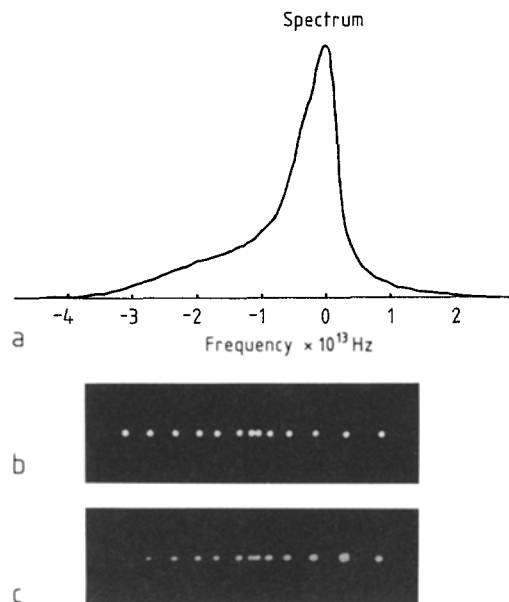


**Fig. 6.** **a** Plot of the spectral intensity  $I_{in}(\omega) = |a_{in}(\omega)|^2$ ; **b** magnified photo of the original image, hole diameter  $70 \mu\text{m}$ ; **c** a reconstructed image: photo from the screen of the monitor

All gratings in the system were holographic, with  $d^{-1} = 1800$  lines per mm, and the angle  $\theta_0$  was chosen about  $75^\circ$ . Two equal Fourier objectives with a focal distance  $f = 18$  cm were used in the transmitter and another with  $f = 25$  cm in the receiver. The image sensor was a CCD camera with  $25 \mu\text{m}$  pixel size. The  $R$  value, calculated with the parameters specified above, was about 340.

Figure 6b presents the magnified photo of an amplitude mask, consisting of a holes with diameters of about  $70 \mu\text{m}$ . The photo of the reconstructed image is shown in Fig. 6c. The distances between the holes are correctly reconstructed, but a change of some hole diameters is observed: the holes placed near the maximum of the spectrum appear larger in the restored image. In fact, in the plane of the sensor  $F'_3$  the holes have equal sizes but different intensities, in accordance with (5) calculated for the our case. However, the threshold of the CCD sensor has been adjusted according to the points with lower intensities, placed at the spectrum wings. For the central points this threshold corresponds to intensities below 0.5, where the spot is wider (see Fig. 5b).

As mentioned previously, in the case of the phase image  $H(\kappa)$  the restoration of the phase can be done using some of the established techniques. However, we made a successful transfer and reconstruction of phase gratings with up to 10 lines per mm without any special design: an intensity modulation, corresponding to  $H(\kappa)$ , appeared in the the sensor plane. In our opinion, the visualization of the phase was caused by two main reasons: 1) Slight defocusing in the image plane [10, 13]; 2) Canceling of the highest spatial frequencies by the optical components [10]. More detailed investigations of this effect will be presented elsewhere.

### 3. Conclusions

In this paper we analyze the possibility of building an all-optical system for image transfer, based on the

frequency modulation of short light pulses. Our considerations show that, if the transferred image [a mask with transparency  $H(\kappa)$ ] is placed in the Fourier plane of the transmitter, the function  $H(\kappa)$  is carried by the spectral structure of the field at the output of the transmitter. After passing some distance through the transmitting medium, the modulated pulse is reversely processed by the receiver and, as was shown, the field at the input of the sensor is proportional to the function  $H(\kappa)$ . It was found that the main limitation is connected with the spatial profile of the modulated field. To assure the successful reconstruction of the image after the propagation to the receiver, the system and mask parameters must be appropriately chosen.

### References

1. C. Froehly, B. Colombeau, M. Vampouille: *Progress in Optics*, ed. by E. Wolf (North-Holland, Amsterdam 1983) pp. 65–153
2. R.N. Thurston, J.P. Heritage, A.M. Weiner, W.J. Tomlinson: *IEEE J. QE-22*, 682–696 (1986)
3. A.M. Weiner, J.P. Heritage: *Rev. Phys. Appl.* **22**, 1619–1628 (1987)
4. A.M. Weiner, J.P. Heritage, E.M. Kirschner: *J. Opt. Soc. Am. B.* **5**, 1563–1572 (1988)
5. A.M. Weiner, J.P. Heritage, J.A. Salehi: *Opt. Lett.* **13**, 300–302 (1988)
6. M.B. Danailov, I.P. Christov: *J. Mod. Opt.* **36**, 725–731 (1989)
7. J.W. Goodman: *Introduction to Fourier Optics* (McGraw-Hill, San Francisco 1968)
8. J. Arnaud: *Beam and Fiber Optics* (Academic, London 1976) Chap. 2
9. O.E. Martinez: *J. Opt. Soc. Am. B.* **3**, 929–934 (1986)
10. M. Born, E. Wolf: *Principles of Optics* 4th ed. (Pergamon, Oxford 1968) Chap. 8
11. J.A. Valdmanis, R.L. Fork: *IEEE J. QE-22*, 112 (1986)
12. N. Michailov, T. Deligeorgiev, V. Petrov, I. Tomov: "Novel Saturable Absorbers for Passive Mode-Locking of Rhodamine 6G dye Laser", to be presented in CLEO '89
13. L.M. Soroko: *Hilbert-Optics* (Nauka, Moscow 1981) in Russian, Chap. 2